

This document is the unedited Author's version of a Submitted Work that was subsequently accepted for publication in ACS Sustainable Chemistry and Engineering, Copyright (c) 2024 The Authors. Published by American Chemical Society after peer review. To access the final edited and published work see <https://doi.org/10.1021/acssuschemeng.4c00935>

Living diatom microalgae for desiccation-resistant electrodes in biophotovoltaic devices

Cesar Vicente-Garcia,[†] Danilo Vona,[‡] Roberta Ragni,[†] Gabriella Buscemi,[†] Matteo Grattieri,[†] Francesco Milano,^{‡,} Gianluca M. Farinola,^{†,*}*

[†] Dipartimento di Chimica, Università degli Studi di Bari “Aldo Moro”, I-70126 Bari, Italy.

[‡] Dipartimento di Scienze del Suolo, della Pianta e degli Alimenti, Università degli Studi di Bari “Aldo Moro”, I-70126 Bari, Italy.

[‡] Istituto di Scienze delle Produzioni Alimentari, Consiglio Nazionale delle Ricerche, I-73100 Lecce, Italy.

KEYWORDS: bio-photoelectrochemical cell, biophotoanodes, photocurrent, diatom microalgae, dryness resistance.

ABSTRACT

Strategies of renewable energy production from photosynthetic microorganisms are gaining great scientific interest as eco-sustainable alternatives to fossil fuel depletion. Green microalgae have been thoroughly investigated as living components to convert solar energy into photocurrent in biophotovoltaic (BPV) cells. Conversely, suitability of diatoms in BPV cells has been almost completely unexplored so far, in spite of being the most abundant class of photosynthetic microorganisms in phytoplankton and of their good adaptability and resistance to harsh environmental conditions, including dehydration, high salinity, nutrient starvation, temperature, or pH changes. Here we demonstrate the suitability of a series of diatom species (*Phaeodactylum tricornutum*, *Thalassiosira weissflogii*, *Fistulifera pelliculosa* and *Cylindrotheca closterium*), to act as biophotoconverter, coating the surface of indium tin oxide photoanodes in a model BPV cell. Effects of light intensity, cells density, total chlorophyll content, and concentration of the electrochemical mediator on photocurrent generation efficiency were investigated. Noteworthy, biophotoanodes coated with *Thalassiosira w.* diatoms are still photoactive after fifteen days of dehydration and four rewetting cycles, contrary to analogue electrodes coated with the model green microalga *Dunaliella tertiolecta*. These results provide the first evidence that diatoms are suitable photosynthetic microorganisms for building up highly desiccation-resistant biophotoanodes for durable BPV devices.

INTRODUCTION

The worldwide energy demand is continuously increasing over the last decades, with a trend expected to rise in the next future.¹ Despite the current huge global efforts, technologies for sustainable energy production from renewable sources are still at an early stage, and green-energy supply is far from the levels achieved by non-renewable sources.² Solar panels, wind turbines, or geothermal stations are beneficial alternatives to fossil fuel-based energy platforms, reducing the exhaust gases release responsible for climate change. Nevertheless, low recyclability and lifespan of materials used for such technologies currently limit their integration into a circular economy approach.³ In the last two decades, Microbial Fuel Cells (MFCs) have emerged as alternative bio-based platforms for green energy or fuel production. MFCs are electrochemical systems powered by redox reactions catalyzed by living organisms that interact with an abiotic interface.⁴ Although artificial materials are still needed to fabricate the electrical and conductive elements of these devices, the photochemical reactions leading to solar energy conversion are carried out by living microorganisms, that represent intrinsically renewable biomaterials optimized by Nature, and available at large scale and low cost.

MFCs based on photosynthetic organisms are also known as bio-photoelectrochemical cells (BPECs), and they avail of whole photosynthetic microorganisms, intact parts such as organelles, or just isolated photosynthetic proteins as the bioactive components.⁵ BPECs based on oxygenic photosynthetic microorganisms, defined as biophotovoltaic (BPV) cells, feature the major

advantage versus other MFCs of electrical power generation through water photolysis, in the absence of exogenous supply of organic nutrients and with concomitant removal of CO₂ from the external environment. The use of intact photosynthetic microorganisms has several advantages, such as enhanced stability or self-replication, but also the drawback of difficult interaction between the biological catalyst and the abiotic electrode interfaces. Hence, BPVs' sustainability and efficiency are strictly dependent on the choice of appropriate microorganisms, and in particular on their electrogenic capacity, affinity with the electrode material, resilience and compatibility with the device working conditions.⁶ Representative examples of organisms used in BPVs include cyanobacteria,⁷ eukaryotic microalgae,⁸ and more recently even macroalgae.⁹

BPVs based on diatom microalgae are currently underrepresented, with very rare investigations reported so far in the literature,^{10,11} despite their interesting characteristics. In fact, diatoms are unicellular photosynthetic microorganisms that represent the most abundant species of phytoplankton. They live in suspension (planktonic diatoms) or adhering to substrates (benthonic diatoms), both in freshwater and marine habitats.¹² With respect to green and red microalgae, diatoms better adapt and survive to environmental changes of salinity,¹³ pH and temperature,¹⁴ due in part to the presence of nanostructured biosilica shells (frustules) that protect cells protoplasm from mechanical, biological, and radiative stress factors, while allowing the free exchange of nutrients and other elements.¹⁵ Being mainly autotrophic, they easily grow even in low-nutrient environments.¹⁴ The broad availability of diatoms in all marine ecosystems also enables them to be cultured under mild conditions and at a large scale, thus envisaging their application as biofactories of high added-value products such as pigments, oils, biofuel,¹⁶ and nanostructured biosilica-based materials for medicine,¹⁷ photonics,¹⁸ optoelectronics,¹⁹ and environmental bioremediation.²⁰ Diatoms also bear profitable features for application in BPEC solar energy

conversion technologies because benthonic microalgae can generate biofilms adhering to a variety of materials,²¹ such as electrodes' surfaces, thus allowing their spontaneous colonization. Their biofilms are also rich in bioactive molecules and proteins,^{22,23} with unexplored electron-transfer potential. In principle, chemical modification of diatoms with tailored materials with conductive properties may be also a powerful tool to face one of the most important challenges in BPV design *i. e.* favoring electrical communication between the biotic (microalgae) and abiotic (electrode) elements.²⁴ Moreover, due to their ability to withstand extreme conditions like water starvation and desiccation,^{25,26} diatoms are promising candidates for BPVs. In fact, whether the bioanode preparation includes a desiccation step, they would not need protection into hydrogels or other encapsulating materials that are conversely essential for dryness suffering species.²⁷ Moreover, persistent light irradiation or aqueous medium evaporation are common issues expected for BPVs working under practical uncontrollable conditions, making crucial the choice of very resistant photosynthetic microorganisms.²⁸ For example, desiccation-resistance of microalgae could enable easy transport and dry state storage. In this way, BPVs could be activated by adding electrolyte, as well as they could be switched-on/off providing or withholding moisture.

Diatoms are expected to have significant electrogenic capacity,¹⁰ since their membrane oxidoreductases enzymes are highly expressed.²⁹ These proteins have important roles in signaling, growth and even interaction of microalgae with other microorganisms. Membrane oxidoreductases with ferrireductase (FR) activity play an important role in electrogenic capacity, being related to the photosynthetic electron transport.³⁰ Moreover, NADPH oxidases are supposed to produce superoxide species outside the cell via plasma membrane electron transport.³¹ Literature also reports that the enhancement of membrane NADPH oxidase activity in *Phaeodactylum tricorutum* diatoms leads to increased photocurrent production in BPVs working with

ferricyanide as an exogenous soluble mediator.¹⁰ On this ground, the high electrogenic capacity and resistance of diatoms to stress conditions are significant features motivating the need of an in-depth investigation of the suitability of these microorganisms as bioactive components in BPVs, these aspects being not yet systematically studied with respect to other microalgae candidates.

Herein we provide a systematic investigation of the performance of diatom-based BPV cells with three-electrode configuration, where an ITO working electrode is coated with a series of diatom species, namely *Phaeodactylum tricornutum*, *Thalassiosira weissflogii*, *Fistulifera pelliculosa* and *Cylindrotheca closterium*. The effects of the electrode coating procedure, deposited cells density, electrochemical mediator concentration, light intensity, and electrochemical potential on the biophotoanode performance have been evaluated to set the best experimental working conditions of the BPV.

To the best of our knowledge, this study provides the first evidence that the biophotoanodes prepared with the model diatom *Thalassiosira weissflogii* keep their photoactivity in BPV cells, resisting to a series of desiccation/rewetting cycles and repeated photocurrent extraction much better than biophotoanodes from the model green *Dunaliella tertiolecta* microalga.

EXPERIMENTAL SECTION

Materials and Reagents

All chemicals were used as received without further purification. Ultrapure grade acetone, ethanol, ferricyanide, K_2HPO_4 , KH_2PO_4 , $K_3[Fe(CN)_6]$ (K-ferricyanide), $K_4[Fe(CN)_6]$ (K-ferrocyanide), *N,N*-Dimethylformamide (DMF), F/2 Guillard concentrate 50x, HellmanexTM III solution and fluorescein diacetate (FDA), were purchased from Sigma Aldrich (Germany). All aqueous

solutions were prepared using deionized water obtained by Milli-Q Gradient A-10 system (Millipore, 18.2 M Ω cm, organic carbon content $\leq 4 \mu\text{g L}^{-1}$). Indium tin oxide (ITO) glass slides of $1.8 \times 0.8 \text{ cm}^2$ area, 0.7 mm thickness, $\sim 60 \Omega \text{ sq}^{-1}$ surface resistivity and a transmittance $> 85\%$ were used for the preparation of bioelectrodes.

Microalgae Growth

Phaeodactylum tricornutum (CCAP strain 1055/1, Pt), *Thalassiosira weissflogii* (CCAP strain 1085/18, Tw, also known as *Conticribra weissflogii*), *Fistulifera pelliculosa* (CCAP strain 1050/9, Fp, formerly known as *Navicula pelliculosa*), *Cylindrotheca closterium* (Nantes Cultures Collection, Cc), and *Dunaliella tertiolecta* (CCAP strain 19/24, Dt) were grown inside a vertical incubator with controlled temperature and relative humidity ($18 \pm 2 \text{ }^\circ\text{C}$, 65%) under a photosynthetically active radiation (PAR) of 20–40 $\mu\text{mol}\cdot\text{m}^{-2}\cdot\text{s}^{-1}$ measured by a MSC15 Spectral Light Meter (Gigahertz Optik, Germany), and provided by two white fluorescent tubes (6500K, 30W) on a 16/8 h light/dark cycle. Cultures were grown in F/2 Guillard prepared with sterile natural seawater (28 practical salinity unit), buffered with 1 mM NaHCO₃ at pH 7.8, in polystyrene flasks (250 mL) without stirring. Half of the culture volume was substituted with fresh medium every 2 weeks, and splitting was performed once a month. Cells used for bioelectrochemical measurements were taken between the late exponential and early stationary growth phases.

Preparation of biophotoanodes

ITO-coated glass slides were used to prepare the microalgae-based bioanodes. Cell density was determined by using a Bürker cell counting chamber. Cells were recovered at $360 \times g$ for 12 min at room temperature (RT). For the preparation of each bioanode, the microalgae pellet was suspended in 20 μL of 90 mM phosphate buffer pH 7.8 (PB), spotted onto ITO slide covering an

area of 0.8 cm^2 ($0.8 \times 1.0 \text{ cm}^2$) prior to air dry (**Figure 1a**). This methodology allows to obtain artificial films of diatoms onto an ITO slide containing a known number of cells (10^6 cells per slide, unless stated otherwise). ITO slides were reused after a thorough washing routine (sonication in 5% HellmanexTM III solution, followed by sonication in deionized water, rinsing with acetone, and finally dried under a fume hood). A Cary 5000 UV-Vis-NIR spectrophotometer (Agilent Technologies Inc. – USA) was used to record the absorbance spectra of the dry biophotoanodes, for the calculation of the Internal Quantum Efficiency (IQE).

Electrochemical setup

All electrochemical measurements were performed using an Autolab potentiostat PGSTAT 10, using a 1 mL polystyrene open photoelectrochemical cell ($1.0 \times 1.0 \times 1.0 \text{ cm}^3$) with a three-electrode configuration, using PB as the electrolyte (**Figure 1b**). The transparent ITO slide coated with the microalgal film was used as the working electrode (WE), performing the anodic reaction, with a submerged area of 0.8 cm^2 . A platinum wire with an 0.314 cm^2 estimated submerged area ($r = 0.05 \text{ cm}$; $h = 1.00 \text{ cm}$) and Ag|AgCl (KCl 3 M) were used as the counter (CE) and reference (RE) electrodes respectively. Potassium ferricyanide was used as soluble electrochemical mediator at 0.5 mM concentration (unless stated differently). To ensure a sufficient overpotential to drive the oxidation reaction of the redox mediator, chronoamperometric measurements (CA) were performed at a potential 0.23 V higher than the half wave potential ($E_{1/2}$) of the ferro/ferricyanide couple. $E_{1/2}$ is evaluated by a cyclic voltammetry ($20 \text{ mV} \cdot \text{s}^{-1}$ fixed speed) immediately prior every CA experiment, to avoid potential undesired variations that may occur upon any change of bioanode (**Figure 1c**). The system was illuminated by a white LED bulb (3000 K, from 425 to 725 nm, with maximum emission peaks at 455 and 600 nm), with a light intensity of $54 \text{ mW} \cdot \text{cm}^{-2}$ at a working distance of 5.5 cm (unless stated differently), measured by a MSC15 Spectral Light Meter

(Gigahertz Optik, Germany). The white LED was purposefully chosen because its emission appropriately fits with the absorption of the microalgae photosynthetic pigments (**Figure S1**). Light/dark cycles of 300 s were applied during CA measurements. The system was unstirred, at 20 - 25 °C and covered by a black velvet fabric to guarantee complete darkness. All CA experiments were performed in triplicate under the following set conditions, unless otherwise stated: 1 mL PB, 0.5 mM K-ferricyanide, $P = E_{1/2}(\text{ferro/ferricyanide}) + 0.23\text{V}$, $54 \text{ mW}\cdot\text{cm}^{-2}$ white light intensity, 4 light cycles of 300 s, 45 min total time under applied potential, RT, unstirred.

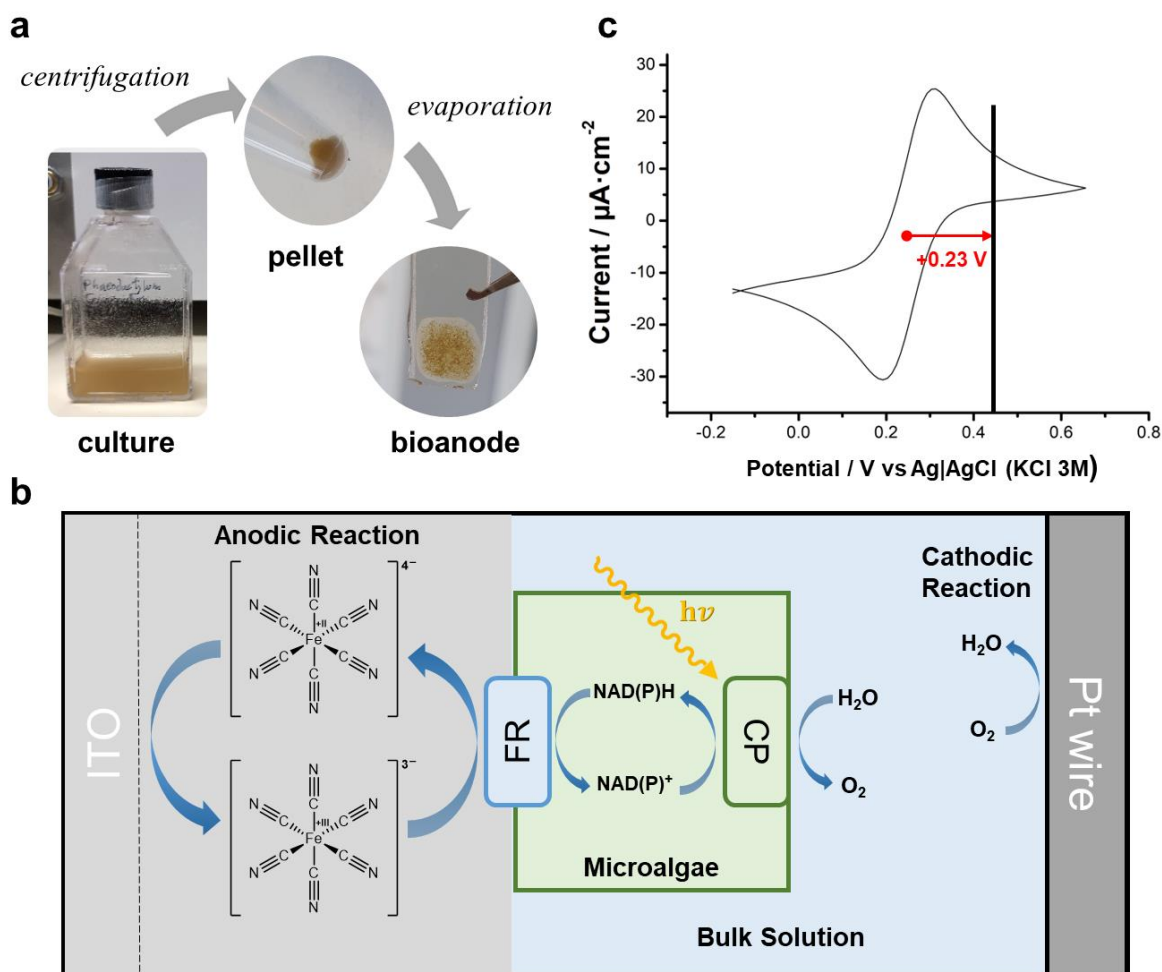


Figure 1. (a) Preparation of the air-dried diatom bioanode from a fresh culture of diatoms. (b) Scheme of the photoelectrochemical cell representing the microalgae-coated ITO WE, the

chloroplast (CP) inside the microalgae, the membrane ferrireductase (FR), the ferro/ferricyanide couple in PB solution, and the platinum wire CE. The reference electrode has not been depicted for simplicity, and the different phases are not in scale. (c) Cyclovoltammetry performed at 20 $\text{mV}\cdot\text{s}^{-1}$ scan rate with ITO electrode coated with 10^6 cells and immersed in a solution containing 0.5 mM K-ferricyanide; the red arrow shows the overpotential of +0.23 V with respect to $E_{1/2}$ of the ferro/ferricyanide couple applied in the CA experiments.

Cell viability studies

Morphology and viability of the cells in liquid cultures, as well as of the cells coating the bioanodes, were checked by means of epifluorescence microscopy with an Axiomat Zeiss microscope (Oberkochen, Germany) using a TRITC filter set, through evaluation of chlorophyll fluorescence of chloroplasts ($\lambda_{\text{ex}} = 568 \text{ nm}$, $\lambda_{\text{em}} > 600 \text{ nm}$). To further evaluate the viability of microalgae before and after the CA measurements, the fluorescein diacetate (FDA) assay was used. FDA is a non-polar, non-fluorescent molecule that can passively diffuse through cellular membranes and accumulate inside cells. Only when in contact with living cells, it can be hydrolyzed by esterases to a green fluorescent derivative exclusively staining the living cells.³² Cells were centrifuged at $360 \times g$ for 12 min at RT and the cell pellet was suspended in 1 mL PBS and a FDA acetone solution (12 μL , 5 mM) was added. The mixture was dark incubated for 1.5 h and transferred to a flat-bottom 96-well transparent plate. Fluorescence intensity at 511 nm was recorded ($\lambda_{\text{ex}} = 488 \text{ nm}$) by a Spark[®] Multimode Microplate Reader (Tecan, Switzerland) and it was used to evaluate and compare the viability of each sample (normalized to 10^6 cells) after subtracting the background signal from the sole buffer and normalizing the highest sample to 100%.³³

Total chlorophyll quantification

For total chlorophyll quantification, fresh samples from each species were used. Cells were stirred in DMF (2 mL DMF/10⁶ cells) at 4 °C in the dark, for 24 h. Cells were then centrifuged for 12 min at 4000 × g. Absorption spectra of the supernatant was recorded in the 250-900 nm range using a Cary 5000 UV-Vis-NIR spectrophotometer (Agilent Technologies Inc. – USA). The total chlorophyll content was calculated as it follows: total chlorophyll (mg·L⁻¹) = 7.74 × A₆₆₄ + 23.39 × A₆₃₀.¹⁰

Statistical analysis

Statistical tests were performed using GraphPad Prism (v.6.0.1). Paired two-tailed Student t test was used for pairwise comparisons, while two-way ANOVA followed by Sidak multiple comparisons test were performed for multiple comparisons. Statistical significance was assessed by using $p < 0.05$. P values lower than 0.01 and 0.001 are marked with two and three asterisks, respectively.

RESULTS AND DISCUSSION

The BPV cell setup was assembled in accordance with a well-known configuration, selecting robust and standard materials that are commonly used in literature for photoelectrochemical systems. Likewise, for the setup optimization, *Phaeodactylum tricornutum* (*Pt*) was selected as the model diatom species to be deposited on the bioanode due to its well-known adaptability and resilience under harsh conditions.¹⁵ Indeed, *Pt* shows several properties desirable for BPV applications, such as the ability to form adhesive biofilms that can colonize the surface of an electrode, as well as the capacity to thrive even under low-nutrient conditions, ensuring long-

lasting cultures.³⁴ Setup parameters optimized using the *Pt*-coated bioanodes were then applied to all experiments carried out with different microalgal species.

Implementation of the photoelectrochemical setup and bioanode fabrication

The photoelectrochemical system was designed to enable the photocurrent extraction from living microalgae with fair efficiency and reproducibility. ITO-covered glass was chosen as the anode due to its good interaction and compatibility with diatom microalgae.³⁵ Cyclovoltammetry of the ferro/ferricyanide couple was carried out to select the appropriate potential to be applied to the WE in the presence of living microalgae. Since the photosynthetic activity of microalgae is expected to reduce ferricyanide, the applied external potential must be selected to re-oxidize ferrocyanide and regenerate the mediator at the surface of the anode (ITO). For this reason, potential for CA was set at +0.23 V vs $E_{1/2}$ of the mediator redox couple.

Adsorption of photosynthetic microorganisms onto the WE surface is a profitable strategy to favor the interaction between electrode, mediators, and living cells involved in the anodic reaction.^{32,36} Indeed, this strategy allows to confine the processes leading to photocurrent next to the bioanode. For this aim, the model *Pt* diatom cells were concentrated into a small volume, drop-casted onto the ITO surface and air-dried at RT. The resulting bioanode coated with 10^6 cells yielded photocurrents with good signal to noise ratio, and good repeatability after the first cycle (~100 nA/cm² at the fourth illumination cycle) (**Figure 2a**, black trace). Conversely, the use of *Pt* cells in suspension produced much lower photocurrents with worse signal to noise ratio (**Figure 2a**, red trace). Time stability of the microalgal film was confirmed by observing that less than 1 % *Pt* cells detach from the bioanode after one CA measurement lasting 45 min (**Figure S2**).

The partial dehydration process used for the bioanode preparation is expected to stress cells. Bright field and fluorescence microscopy images of the bioanode were acquired to evaluate cell viability before and after CA measurements. The strong red fluorescence, upon green light excitation of chlorophylls, confirmed chloroplast integrity (**Figure 2b**),³⁷ indicating that *Pt* diatoms are still intact after being subjected to an overall 45 min experiment of photocurrent extraction in the presence of ferricyanide mediator, including four photoexcitation cycles (5 min light / 5 min dark each). This outcome further confirms the ability of *Pt* diatoms to interact with ferricyanide as previously reported in literature.¹⁰ This result is also supported by the FDA viability test, which shows no significant differences in viability of *Pt* cells before and after the CA measurement (**Figure 2c**).

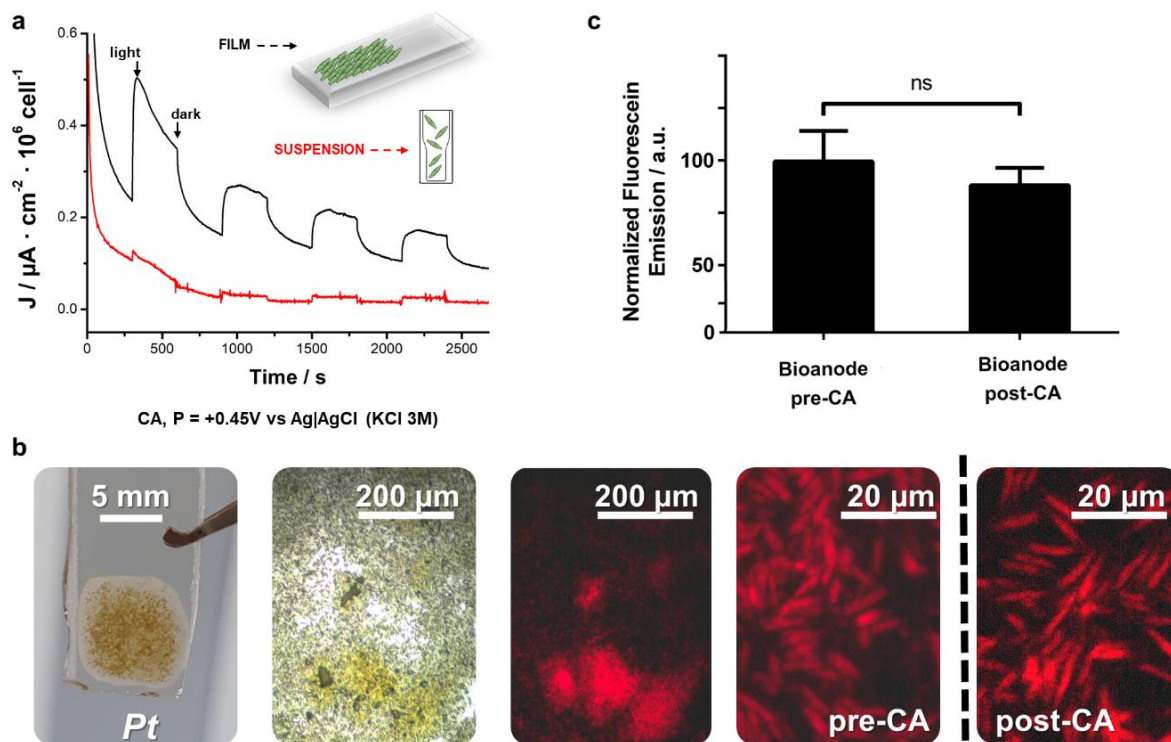


Figure 2. (a) Photocurrent signals from 10^6 *Pt* cells in suspension (red), and 10^6 *Pt* cells coated ITO bioanode (black). (b) Images of a *Pt* coated ITO bioanode, from left to right: macroscopic

view, bright field microscopy image at 20x, fluorescence microscopy images ($\lambda_{\text{ex}} = 568 \text{ nm}$, $\lambda_{\text{em}} > 600 \text{ nm}$) at 20x, at 100x before CA, at 100x after CA. (c) Mean fluorescein emission ($\lambda_{\text{ex}} = 488 \text{ nm}$, $\lambda_{\text{em}} = 511 \text{ nm}$) in the FDA viability assay of *Pt* cells performed before and after CA.

Photocurrent dependence on living cell photosynthetic activity and setup optimization

To demonstrate the key roles of the viable photosynthetic cells deposited onto ITO and of the ferricyanide mediator, a series of control experiments were performed. Upon using a bare ITO electrode instead of the *Pt* coated analogue, no photocurrent was observed (**Figure 3a**, blue line), thus excluding any contribution from the sole mediator. The same result was obtained when the bioanode was prepared using *Pt* cells thermally inactivated at 120 °C (**Figure 3a**, black line). Moreover, in the absence of ferricyanide mediator, only a small photocurrent signal was observed (**Figure 3a**, green line, inset). This indicates that the soluble mediator is the main species responsible for the extracellular electron transfer between diatoms and the electrode under the conditions studied. However, the presence of a non-negligible photoresponse from the bioanode without the external mediator, despite being of low intensity, suggests the presence of redox active metabolites suitable as endogenous mediators enabling electron transfer from cells to the electrode (**Figure 3a**, inset). Redox active biological molecules that facilitate electron transfer have been already described for photosynthetic microorganisms, like endogenous quinones or NADPH.²⁴ A direct electron transfer from diatom cells to ITO seems unlikely since no natural conductive structures have been previously described for diatoms. However, the presence of endogenous mediators cannot be completely ruled out, since the biosilica is enfolded in a complex network of biomolecules, including polyphenols and NADPH, that could potentially possess some electron transfer capabilities.^{22,38} Moreover, electron transfer can occur via extracellular material secreted by biofilm-forming photosynthetic microorganisms like cyanobacteria,³⁶ a property that could be

shared by a benthonic diatom such as *Pt*. Even though the bioanode used constitutes an artificial film and is not a natural biofilm, extracellular material is likely entrapped in the *Pt* pellet that serves as starting material for the bioanode fabrication. Therefore, despite being of low intensity, the photocurrent signal reported in the inset of **Figure 3a** is interesting, since it suggests the possibility to avoid the use of an external mediator if biotechnological methods are employed to boost production of endogenous mediators by cells.

The photocurrent output of BPV cells depends on both intensity and emission spectrum profile of the light source.²⁷ In our experiment a white LED (emission spectrum in **Figure S1**) was chosen since its emission fits with the absorption of the microalgae photosynthetic pigments. By tuning the distance between the BPV cell and the LED, three different irradiance values (10, 30 and 54 mW/cm²) were set according to the values commonly used for BPVs characterization.³⁹ The photocurrent output upon illumination at different light intensity is shown in **Figure 3b**. A rough linear trend can be observed and no plateau was reached, this showing that light intensity is still sub-saturating at the highest irradiance used. This result demonstrates that photocurrent generation by *Pt* diatoms can be enhanced by increasing light intensity, without perturbing the living cells.

The fabrication of an artificial film of diatoms enables to study the effect of cell density of the deposited *Pt* cells on the photocurrent output. When increasing cell density on the WE surface a significant increase of photocurrent can be observed (**Figure 3c**). However, doubling the cell density does not lead to a doubled value of photocurrent; this suggests that cells closer to the surface of the electrode may transfer electrons more efficiently via the soluble mediator than cells located in more external layers of the film.

Figure 3d shows the photocurrent trend versus the concentration of the ferricyanide mediator. A roughly linear trend is observed up to 250 μM concentration, after which a plateau is reached. The ferricyanide concentration of 250 μM is sensibly lower than that (1 mM) reported in literature for a similar setup based on the same microalgal species in suspension.¹⁰ This is a relevant advantage since exogenous mediators such as ferricyanide compromise cells viability if used at high concentration.⁴⁰

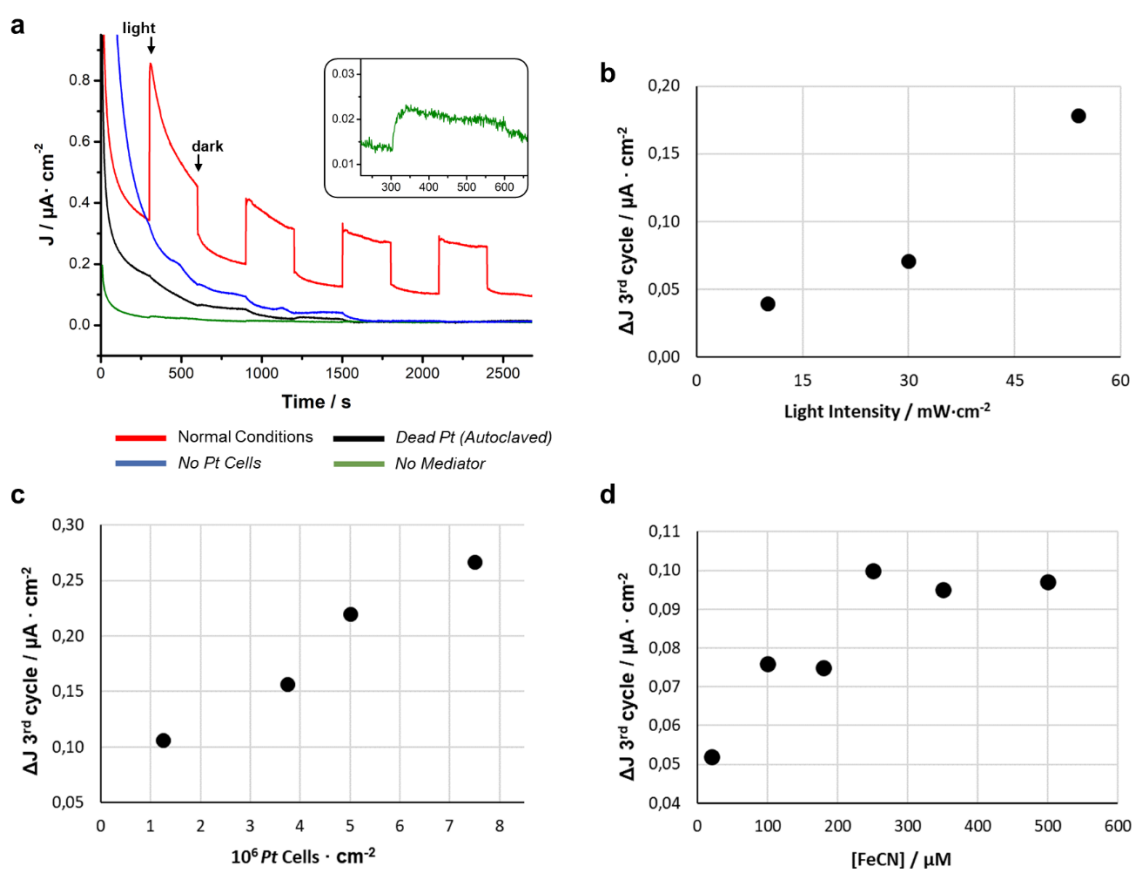


Figure 3. (a) Photocurrent measurements carried out: under the standard conditions reported in the experimental (red line); using bare ITO as WE (blue line); in the absence of ferricyanide mediator (green line); using Pt cells after an autoclave cycle (121 °C, 15 psi, 20 min). Inset: detail of photocurrent signal from Pt in the absence of ferricyanide. Photocurrent values on the third

cycle of illumination at increasing (b) light intensity (10, 30 and 54 mW·cm⁻²), (c) cell density of *Pt* cells onto ITO surface, and (d) concentration of ferricyanide mediator.

Photocurrent generation efficiency of different diatom species

After setting the conditions to obtain bioanodes coated with the model *Pt* cells and to use them as WEs in BPV cells, a comparative study was carried out to evaluate photocurrent generation efficiencies of different diatom species that share common features suitable for their processability onto bioanodes but differ in lifestyle (benthonic, planktonic, or mixed), size, pigment content and frustule shape. Photocurrent output is expected to depend to some extent on specific cell features. For this aim, three further diatom species were selected as counterparts to the model *Pt*: the benthonic pinnates (i) *Fistulifera pelliculosa* (*Fp*) and (ii) *Cylindrotheca closterium* (*Cc*), the planktonic, centric (iii) *Thalassiosira weissflogii* (*Tw*) with sizes smaller, slightly larger, and much larger than *Pt*, respectively. Pinnate *Fp* and *Cc* were investigated versus pinnate *Pt* to evaluate possible effects of different sizes, number of chloroplasts per cell and chlorophyll overall content, on photocurrent. Moreover, the centric *Tw* was studied to compare its photoelectrochemical response with that of pinnate species. *Tw* is much larger than the other selected diatoms, showing a higher chlorophyll content due to its higher number of chloroplasts (~8-12 for *Tw* cell vs 1 for *Fp* or *Pt* and 2 for *Cc*).

Bright field and fluorescence images ($\lambda_{\text{ex}} = 488 \text{ nm}$, $\lambda_{\text{em}} = 511 \text{ nm}$) were acquired to observe both single diatom cells (**Figure 4a**) and their films onto electrodes (**Figure S3**), to evaluate their morphological features and viability. Individual cells and the typical red fluorescence of chlorophyll were observed in all cases.

Figure 4b and **4c** show the photocurrent density output recorded at the 3rd illumination cycle for the four different diatoms species, and the total chlorophyll amount (expressed as μg per 10^6 cells), respectively. Increasing the size of pinnate species ($Fp < Pt < Cc$), a clear increase of photocurrent density (**Figure 4b**) and the total chlorophyll amount (**Figure 4c**) can be observed, and a linear trend of the photocurrent density versus the total chlorophyll amount is evidenced in **Figure 4d** (dotted line). Conversely, *Tw* bears an expected higher content of chlorophyll, and yet a photocurrent density comparable to that of *Cc*. Such effect may be related to a larger surface to volume ratio in the case of *Tw*, in which chloroplasts can be located far from the external cell membrane, limiting their contribution to the photocurrent generation. Such differences may also arise from other key parameters like the species-specific content of enzymes and cofactors involved in intracellular electron transport or in the interaction with the mediator. Hence, the intracellular location, chlorophyll content and number of chloroplasts may play a relevant role on the ability of diatoms to generate photocurrent, with pinnate diatoms bearing more dense regions of chloroplasts next to the external membrane performing similarly to larger centric diatoms.

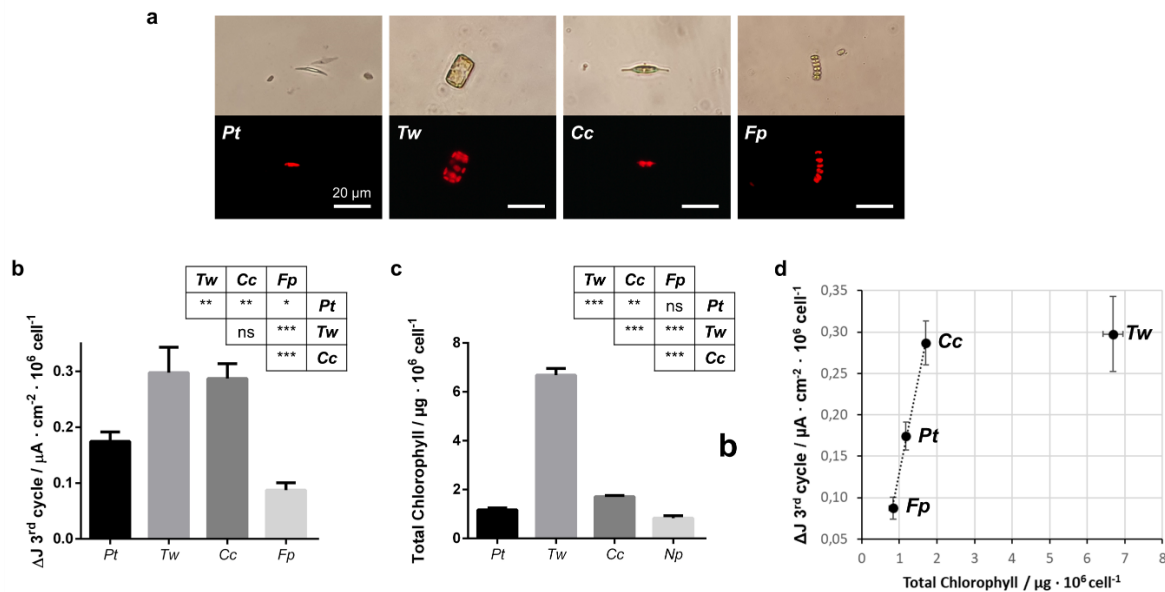


Figure 4. (a) Bright field images of the studied diatom species at 100x on top, and chloroplast fluorescence images at the bottom. The number of chloroplasts per cell is visible for every single cell (except for *Fp*, which appears as a chain-like colony of single cells). Scale bar corresponds to 20 μm . (b) Average photocurrent density at the third light cycle from the different species studied, normalized to the number of cells onto the bioanode. (c) Total chlorophyll content of each species. Tables report the pairwise tests showing the statistical differences in the chlorophyll content and photocurrent output for the investigated species. (d) Photocurrent values of different species of diatoms on the third cycle of illumination and under the set conditions, plotted versus the average total chlorophyll content of each species, normalized to 10^6 cells. A linear tendency is appreciated between the biofilm-forming species *Fp*, *Pt*, and *Cc*.

The integrity of the films obtained from different species was evaluated by counting the number of cells detached from the film into the solution after a 45 min CA measurement. The average number of detached cells was lower than 2.5% for all species with the exception of *Fp* (lower than 5.0%, **Figure S2**), this meaning that detachment does not significantly affect the differences in maximum photocurrent output between species. Therefore, *Tw* and *Cc* large species significantly overperform the photocurrent generation of both smaller size *Pt* and *Fp*.

***Tw* displays a higher resistance to repeated photocurrent extraction than a model green Microalga**

Photocurrent generation efficiency of a diatom species was also compared to that of the model green microalgal species *Dunaliella tertiolecta* (*Dt*) already reported in the literature to produce biophotoanodes in BPVs.^{41,42} *Dt* was also selected as a marine microalga with well-known endurance to drying and halotolerance.⁴³ *Tw* has several similarities with *Dt* in terms of cell size

(**Figure S4a**), and marine planktonic behavior. Upon the same conditions used for diatoms (see *Materials and Methods*), a photocurrent density of $0.22 \pm 0.04 \mu\text{A cm}^{-2}$ was detected for *Dt* coated biophotoanodes in BPVs (**Figure S4**, left), this being slightly lower than the values recorded for *Cc* and *Tw* and higher than *Pt* and *Fp* counterparts (**Figure 4b**). Moreover, *Dt* showed an overall chlorophyll content of $\sim 3 \mu\text{g} \cdot 10^{-6} \text{ cells}^{-1}$ (**Figure S4b**, right), being higher than *Pt*, *Fp* and *Cc* content and lower than the value recorded for *Tw* (**Figure 4c**).

Two different comparative investigations were carried out for *Tw* and *Dt* coated biophotoanodes. In the first experiment, three sets of bioanodes were fabricated for both *Tw* and *Dt* cells (9 electrodes per each species, to ensure the analysis in triplicate). Each set was stored in dry state at room temperature and indoor ambient light. Photocurrent output of the first set was evaluated immediately after its fabrication, while the second and the third sets of dried electrodes were tested three and nine days after their fabrication, respectively, to evaluate how long-term storage of microalgae kept under dryness can influence their photocurrent generation efficiency over time.

Figure 5a shows that photocurrent values of both species remained almost unchanged in the period of time studied, with the differences in their output being not statistically significant. Therefore, this first experiment did not evidence a significant difference in performance of *Tw* diatom versus *Dt* green microalga.

As further comparative investigation, a second experiment was carried out measuring photocurrent densities from two sets (3 electrodes per set for triplicate analysis) of *Tw* and *Dt* coated biophotoanodes subjected to a drying/wetting cycle between every CA consecutive measurement. In this case, each electrode was used for CA measurements over 15 days. CA was carried out immediately after the dryness step needed for the electrode preparation (time = 0). Then, the

electrode was dried and stored at room temperature for three days, after which the electrode was rewetted by immersion into the BPV cell for the second CA. Re-drying and dry-storage was repeated twice for further six days, thus performing further CAs at the 9th and 15th days from the electrode fabrication, to evaluate the photocurrent output and resistance of cells versus prolonged storage time and re-use in a BPV device.

On day 0, the average *Tw* and *Dt* photocurrents were similar to those recorded in the first experiment. On day 3, photocurrent recorded for *Tw* remained unchanged ($98 \pm 5\%$), while *Dt* photocurrent significantly decreased to $60 \pm 3\%$ versus the value at time 0 (**Figure 5b**). After 9 to 15 days, *Tw* photocurrent gradually decreased to $66 \pm 7\%$ and $30 \pm 3\%$, respectively. Conversely, *Dt* photocurrent dropped to an undetectable value already at the 9th day. This comparative result with respect to a well-known green microalgal species *Dunaliella tertiolecta*, strengthens the evidence that diatoms microalgae, such as *Thalassiosira weissflogii*, are very promising candidates for biophotovoltaic applications.²⁸

Higher resistance to drying/wetting cycles of diatoms versus green microalgae might be related to diatoms peculiar mesoporous biosilica shells that protect their organic protoplasm from external noxious factors and stress, such as exogenous viruses or aggressive chemicals, persistent or intense UV-blue light irradiation, and limited water availability. Further aspects that might differently affect the photocurrent response of the two microalgal species over time are the application of external potential and the presence of an exogenous soluble mediator in the BPV cell. However, these hypotheses require further investigation to shed light on the effective factors responsible for the higher resistance to dryness of *Tw* diatoms versus the green *Dt* cells.

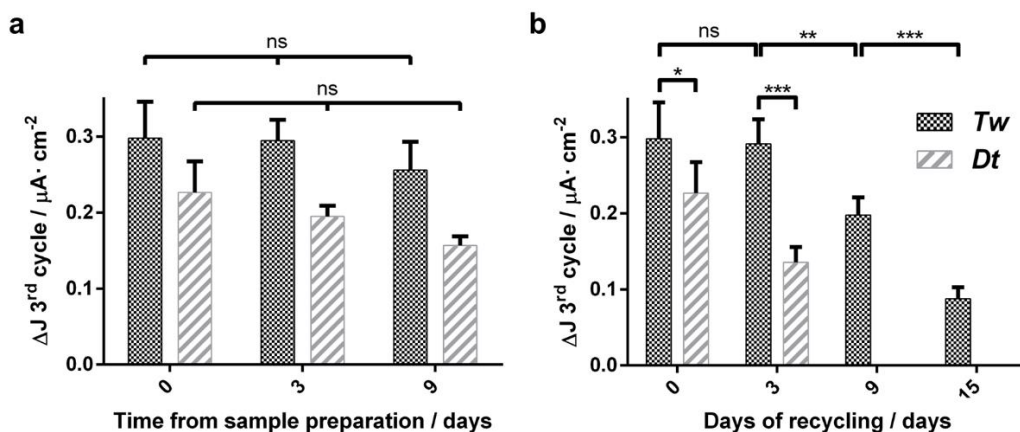


Figure 5. Photocurrent values on the third cycle of illumination under the set conditions, for (a) *Tw* and *Dt* biophotoanodes after a different number of storage days in dry state. (b) *Tw* diatoms and green *Dt* based biophotoanodes, re-used for photocurrent extraction four times over a period of 15 days.

Internal Quantum Efficiency of BPVs

The Internal Quantum Efficiency (IQE), defined as the ratio between the number of electrons pumped into the circuit and the number of photons transferred to the anode,⁴⁴ is a common figure of merit for BPVs. For IQE calculation (**Equations S1-S5**), a monochromatic lighting source was required to evaluate the number of photons radiating cells.⁴¹ For this aim, a red LED emitting at 660 nm with full width at half maximum of 40 nm was used (**Figure S1**). IQE values of $0.072 \pm 0.015 \%$ and $0.026 \pm 0.007 \%$ were obtained under the standard conditions for *Tw* and *Dt*, respectively. This result is another proof that *Tw* overperforms *Dt* in a BPV. Moreover, the IQE for *Tw* is similar to that reported in the literature for optimized BPV devices based on cyanobacteria,⁴¹ and considering that our BPV setup was selected to be as simple as possible, such a similarity highlights the effective suitability of diatoms as candidates of election for the fabrication of efficient BPVs.

CONCLUSION

In summary, diatoms are valuable candidates for the fabrication of biophotoanodes in BPVs, with photocurrent generation efficiencies depending on the microalgal species used to coat the electrode, as well as on the intensity of lighting source and on the cell density at the bioanode surface. A linear trend of photocurrent is observed increasing light intensity, this showing that the highest irradiance used ($54 \text{ mW}\cdot\text{cm}^2$) is still sub-saturating and does not alter living cells. A linear increase of photocurrent is also observed when increasing cell density on the WE surface, with photocurrent values likely being more dependent on number of cells in close contact with the electrode. A further advantage observed for biophotoanodes based on diatoms is that BPVs require lower amount of mediator with respect to already reported bioanodes working with different photosynthetic microorganisms such as bacteria.⁴⁰

Our study also evidences that the photocurrent output of BPVs based on different diatom species varies depending on the total chlorophyll content per cell, with the best results recorded for *Thalassiosira weissflogii* and *Cylindrotheca closterium* with respect to *Phaeodactylum tricornutum* and *Fistulifera pelliculosa* species.

Moreover, for the first time we have demonstrated a valuable resistance to dryness of biophotoanodes made with *Thalassiosira weissflogii* diatoms versus *Dunaliella tertiolecta* green microalgae, this paving the way for the fabrication of highly robust diatom-based biophotovoltaic devices whose electrodes can be stored for long time under water starvation without altering their efficiency after wetting. This finding is of critical relevance, since desiccation resistance and prolonged use are valued properties of stable living biophotoanodes, for applications ranging from photocurrent production to biosensing.

Future work will be focused on the optimization of the simple BPV configuration studied herein. Possible strategies to optimize device performances include the use of highly nanoporous electrodes to increase their available electroactive surface, the incorporation of diatoms in redox polymers, the selection of the best redox mediators, or even the development of methods avoiding mediators, as well as the use of cell culture medium as the electrolyte to promote diatoms growth directly inside BPVs.

ASSOCIATED CONTENT

Supporting Information. Light emission spectra from different light sources used, average number of fallen cells from bioanodes after CA, morphological analysis of biophotoanodes, morphological information, photocurrent, and chlorophyll content from *Dunaliella tertiolecta*, and equations needed to calculate the IQE.

AUTHOR INFORMATION

Corresponding Author

Francesco Milano, Strada Provinciale Lecce-Monteroni, I-73100 Lecce, Italy, Orcid: 0000-0001-5453-2051, email: francesco.milano@cnr.it,

Gianluca M. Farinola, Via Orabona 4, I-70126 Bari, Italy, Orcid: 0000-0002-1601-2810, email: gianluccamaria.farinola@uniba.it

Author Contributions

The manuscript was written through contributions of all authors. All authors have given approval to the final version of the manuscript.

Funding Sources

This work was supported by H2020-MSCA-ITN-2019 project 860125-BEEP (Bioinspired and bionic materials for enhanced photosynthesis).

ACKNOWLEDGMENTS

The Authors thank Prof. Bruno Freire Boa de Jesus from the Nantes Université for generously supplying the *Cylindrotheca closterium* diatom strain; Dr. Giusy D'Attoma for her help in the viability assay; and Dr. Gabriella Leone for preliminary experiments on diatoms cultures.

ABBREVIATIONS

BPV, biophotovoltaic. *Pt*, *Phaeodactylum tricornutum*. *Tw*, *Thalassiosira weissflogii*. *Fp*, *Fistulifera pelliculosa*. *Cc*, *Cylindrotheca closterium*. *Dt*, *Dunaliella tertiolecta*. MFC, Microbial fuel cell. *BPEC*, Biophotoelectrochemical cell. FR, Ferrireductase. ITO, Indium tin oxide. FDA, Fluorescein diacetate. PAR, Photosynthetically active radiation. RT, Room temperature. PB, Phosphate buffer. IQE, Internal quantum efficiency. CA, chronoamperometry. DMF, Dimethylformamide.

REFERENCES

- (1) Hughes, S. R.; Jones, M. A. *The Global Demand for Biofuels and Biotechnology-Derived Commodity Chemicals*; **2020**. <https://doi.org/10.1002/9781119152057.ch7>.
- (2) Moriarty, P.; Honnery, D. Review: Renewable Energy in an Increasingly Uncertain Future. *Appl. Sci.* **2023**, *13* (1), 388. <https://doi.org/10.3390/app13010388>.

- (3) Gallagher, J.; Basu, B.; Browne, M.; Kenna, A.; McCormack, S.; Pilla, F.; Styles, D. Adapting Stand-Alone Renewable Energy Technologies for the Circular Economy through Eco-Design and Recycling. *J. Ind. Ecol.* **2019**, *23* (1), 133–140. <https://doi.org/10.1111/jiec.12703>.
- (4) Santoro, C.; Arbizzani, C.; Erable, B.; Ieropoulos, I. Microbial Fuel Cells: From Fundamentals to Applications. A Review. *J. Power Sources* **2017**, *356*, 225–244. <https://doi.org/10.1016/j.jpowsour.2017.03.109>.
- (5) Beaver, K.; Gaffney, E. M.; Minteer, S. D. Understanding Metabolic Bioelectrocatalysis of the Purple Bacterium *Rhodobacter Capsulatus* through Substrate Modulation. *Electrochim. Acta* **2022**, *416* (February), 140291. <https://doi.org/10.1016/j.electacta.2022.140291>.
- (6) Shlosberg, Y.; Schuster, G.; Adir, N. Harnessing Photosynthesis to Produce Electricity Using Cyanobacteria, Green Algae, Seaweeds and Plants. *Front. Plant Sci.* **2022**, *13* (July), 1–15. <https://doi.org/10.3389/fpls.2022.955843>.
- (7) Bombelli, P.; Savanth, A.; Scarampi, A.; Rowden, S. J. L.; Green, D. H.; Erbe, A.; Årstøl, E.; Jevremovic, I.; Hohmann-Marriott, M. F.; Trasatti, S. P.; et al. Powering a Microprocessor by Photosynthesis. *Energy Environ. Sci.* **2022**, *15* (6), 2529–2536. <https://doi.org/10.1039/d2ee00233g>.
- (8) Roxby, D. N.; Yuan, Z.; Krishnamoorthy, S.; Wu, P.; Tu, W. C.; Chang, G. E.; Lau, R.; Chen, Y. C. Enhanced Biophotocurrent Generation in Living Photosynthetic Optical Resonator. *Adv. Sci.* **2020**, *7* (11), 1–8. <https://doi.org/10.1002/advs.201903707>.
- (9) Shlosberg, Y.; Krupnik, N.; Tóth, T. N.; Eichenbaum, B.; Meirovich, M. M.; Meiri, D.;

- Yehezkeli, O.; Schuster, G.; Israel, Á.; Adir, N. Bioelectricity Generation from Live Marine Photosynthetic Macroalgae: Bioelectricity from Macroalgae. *Biosens. Bioelectron.* **2022**, *198* (November 2021). <https://doi.org/10.1016/j.bios.2021.113824>.
- (10) Laohavisit, A.; Anderson, A.; Bombelli, P.; Jacobs, M.; Howe, C. J.; Davies, J. M.; Smith, A. G. Enhancing Plasma Membrane NADPH Oxidase Activity Increases Current Output by Diatoms in Biophotovoltaic Devices. *Algal Res.* **2015**, *12*, 91–98. <https://doi.org/10.1016/j.algal.2015.08.009>.
- (11) Khan, M. J.; Das, S.; Vinayak, V.; Pant, D.; Ghangrekar, M. M. Live Diatoms as Potential Biocatalyst in a Microbial Fuel Cell for Harvesting Continuous Diafuel, Carotenoids and Bioelectricity. *Chemosphere* **2022**, *291* (P1), 132841. <https://doi.org/10.1016/j.chemosphere.2021.132841>.
- (12) Malviya, S.; Scalco, E.; Audic, S.; Vincent, F.; Veluchamy, A.; Poulain, J.; Wincker, P.; Iudicone, D.; De Vargas, C.; Bittner, L.; et al. Insights into Global Diatom Distribution and Diversity in the World's Ocean. *Proc. Natl. Acad. Sci. U. S. A.* **2016**, *113* (11), E1516–E1525. <https://doi.org/10.1073/pnas.1509523113>.
- (13) Leterme, S. C.; Prime, E.; Mitchell, J.; Brown, M. H.; Ellis, A. V. Diatom Adaptability to Environmental Change: A Case Study of Two *Cocconeis* Species from High-Salinity Areas. *Diatom Res.* **2013**, *28* (1), 29–35. <https://doi.org/10.1080/0269249X.2012.734530>.
- (14) Zhao, P.; Gu, W.; Wu, S.; Huang, A.; He, L.; Xie, X.; Gao, S.; Zhang, B.; Niu, J.; Peng Lin, A.; et al. Silicon Enhances the Growth of *Phaeodactylum Tricornutum* Bohlin under Green Light and Low Temperature. *Sci. Rep.* **2014**, *4*. <https://doi.org/10.1038/srep03958>.

- (15) Dhaouadi, F.; Awwad, F.; Diamond, A.; Desgagné-Penix, I. Diatoms' Breakthroughs in Biotechnology: <I>Phaeodactylum Tricornutum</I> as a Model for Producing High-Added Value Molecules. *Am. J. Plant Sci.* **2020**, *11* (10), 1632–1670. <https://doi.org/10.4236/ajps.2020.1110118>.
- (16) Vinayak, V.; Khan, M. J.; Varjani, S.; Saratale, G. D.; Saratale, R. G.; Bhatia, S. K. Microbial Fuel Cells for Remediation of Environmental Pollutants and Value Addition: Special Focus on Coupling Diatom Microbial Fuel Cells with Photocatalytic and Photoelectric Fuel Cells. *J. Biotechnol.* **2021**, *338* (July), 5–19. <https://doi.org/10.1016/j.jbiotec.2021.07.003>.
- (17) Cicco, S. R.; Vona, D.; Leone, G.; De Giglio, E.; Bonifacio, M. A.; Cometa, S.; Fiore, S.; Palumbo, F.; Ragni, R.; Farinola, G. M. In Vivo Functionalization of Diatom Biosilica with Sodium Alendronate as Osteoactive Material. *Mater. Sci. Eng. C* **2019**, *104* (June), 109897. <https://doi.org/10.1016/j.msec.2019.109897>.
- (18) Ragni, R.; Cicco, S. R.; Vona, D.; Farinola, G. M. Multiple Routes to Smart Nanostructured Materials from Diatom Microalgae: A Chemical Perspective. *Adv. Mater.* **2018**, *30* (19), 1–23. <https://doi.org/10.1002/adma.201704289>.
- (19) Jeffryes, C.; Campbell, J.; Li, H.; Jiao, J.; Rorrer, G. The Potential of Diatom Nanobiotechnology for Applications in Solar Cells, Batteries, and Electroluminescent Devices. *Energy and Environmental Science*. 2011, pp 3930–3941. <https://doi.org/10.1039/c0ee00306a>.
- (20) Vona, D.; Cicco, S. R.; Labarile, R.; Flemma, A.; Garcia, C. V.; Giangregorio, M. M.;

- Cotugno, P.; Ragni, R. Boronic Acid Moieties Stabilize Adhesion of Microalgal Biofilms on Glassy Substrates: A Chemical Tool for Environmental Applications. *ChemBioChem* **2023**. <https://doi.org/10.1002/cbic.202300284>.
- (21) Tong, C. Y.; Derek, C. J. C. Biofilm Formation of Benthic Diatoms on Commercial Polyvinylidene Fluoride Membrane. *Algal Res.* **2021**, *55* (February), 102260. <https://doi.org/10.1016/j.algal.2021.102260>.
- (22) Gügi, B.; Costauouec, T. Le; Burel, C.; Lerouge, P.; Helbert, W.; Bardor, M. Diatom-Specific Oligosaccharide and Polysaccharide Structures Help to Unravel Biosynthetic Capabilities in Diatoms. *Marine Drugs*. **2015**, pp 5993–6018. <https://doi.org/10.3390/md13095993>.
- (23) Ciglencečki, I.; Dautović, J.; Cvitešić, A.; Pletikapić, G. Production of Surface Active Organic Material and Reduced Sulfur Species during the Growth of Marine Diatom *Cylindrotheca Closterium*. *Croat. Chem. Acta* **2018**, *91* (4), 455–461. <https://doi.org/10.5562/cca3433>.
- (24) Torquato, L. D. de M.; Grattieri, M. Photobioelectrochemistry of Intact Photosynthetic Bacteria: Advances and Future Outlook. *Curr. Opin. Electrochem.* **2022**, *34*, 101018. <https://doi.org/10.1016/j.coelec.2022.101018>.
- (25) Gupta, S.; Agrawal, S. C. Survival and Motility of Diatoms *Navicula Grimmei* and *Nitzschia Palea* Affected by Some Physical and Chemical Factors. *Folia Microbiol. (Praha)*. **2007**, *52* (2), 127–134. <https://doi.org/10.1007/BF02932151>.
- (26) Souffreau, C.; Vanormelingen, P.; Verleyen, E.; Sabbe, K.; Vyverman, W. Tolerance of Benthic Diatoms from Temperate Aquatic and Terrestrial Habitats to Experimental

- Desiccation and Temperature Stress. *Phycologia* **2010**, *49* (4), 309–324.
<https://doi.org/10.2216/09-30.1>.
- (27) Sawa, M.; Fantuzzi, A.; Bombelli, P.; Howe, C. J.; Hellgardt, K.; Nixon, P. J. Electricity Generation from Digitally Printed Cyanobacteria. *Nat. Commun.* **2017**, *8* (1), 1–9.
<https://doi.org/10.1038/s41467-017-01084-4>.
- (28) Gacitua, M.; Urrejola, C.; Carrasco, J.; Vicuña, R.; Srain, B. M.; Pantoja-Gutiérrez, S.; Leech, D.; Antiochia, R.; Tasca, F. Use of a Thermophile Desiccation-Tolerant Cyanobacterial Culture and Os Redox Polymer for the Preparation of Photocurrent Producing Anodes. *Front. Bioeng. Biotechnol.* **2020**, *8* (August), 1–11.
<https://doi.org/10.3389/fbioe.2020.00900>.
- (29) Kustka, A. B.; Shaked, Y.; Milligan, A. J.; King, D. W.; Morel, F. M. M. Extracellular Production of Superoxide by Marine Diatoms: Contrasting Effects on Iron Redox Chemistry and Bioavailability. *Limnol. Oceanogr.* **2005**, *50* (4), 1172–1180.
<https://doi.org/10.4319/lo.2005.50.4.1172>.
- (30) Carmel, N.; Tel-Or, E.; Chen, Y.; Pick, U. Iron Uptake Mechanism in the Chrysophyte Microalga *Dinobryon*. *J. Plant Physiol.* **2014**, *171* (12), 993–997.
<https://doi.org/10.1016/j.jplph.2014.03.014>.
- (31) Anderson, A.; Laohavisit, A.; Blaby, I. K.; Bombelli, P.; Howe, C. J.; Merchant, S. S.; Davies, J. M.; Smith, A. G. Exploiting Algal NADPH Oxidase for Biophotovoltaic Energy. *Plant Biotechnol. J.* **2016**, *14* (1), 22–28. <https://doi.org/10.1111/pbi.12332>.
- (32) Buscemi, G.; Vona, D.; Stufano, P.; Labarile, R.; Cosma, P.; Agostiano, A.; Trotta, M.;

- Farinola, G. M.; Grattieri, M. Bio-Inspired Redox-Adhesive Polydopamine Matrix for Intact Bacteria Biohybrid Photoanodes. *ACS Appl. Mater. Interfaces* **2022**, *14* (23), 26631–26641. <https://doi.org/10.1021/acsami.2c02410>.
- (33) Garvey, M.; Moriceau, B.; Passow, U. Applicability of the FDA Assay to Determine the Viability of Marine Phytoplankton under Different Environmental Conditions. *Mar. Ecol. Prog. Ser.* **2007**, *352*, 17–26. <https://doi.org/10.3354/meps07134>.
- (34) Vona, D.; Ragni, R.; Altamura, E.; Albanese, P.; Giangregorio, M. M.; Cicco, S. R.; Farinola, G. M. Light-emitting Biosilica by in Vivo Functionalization of *Phaeodactylum Tricornutum* Diatom Microalgae with Organometallic Complexes. *Appl. Sci.* **2021**, *11* (8). <https://doi.org/10.3390/app11083327>.
- (35) Ng, F. L.; Phang, S. M.; Periasamy, V.; Yunus, K.; Fisher, A. C. Evaluation of Algal Biofilms on Indium Tin Oxide (ITO) for Use in Biophotovoltaic Platforms Based on Photosynthetic Performance. *PLoS One* **2014**, *9* (5). <https://doi.org/10.1371/journal.pone.0097643>.
- (36) Tucci, M.; Bombelli, P.; Howe, C. J.; Vignolini, S.; Bocchi, S.; Schievano, A. A Storable Mediatorless Electrochemical Biosensor for Herbicide Detection. *Microorganisms* **2019**, *7* (12), 1–14. <https://doi.org/10.3390/microorganisms7120630>.
- (37) Bermejo, E.; Filali, R.; Taidi, B. Microalgae Culture Quality Indicators: A Review. *Crit. Rev. Biotechnol.* **2021**, *41* (4), 457–473. <https://doi.org/10.1080/07388551.2020.1854672>.
- (38) Rico, M.; López, A.; Santana-Casiano, J. M.; González, A. G.; González-Dávila, M. Variability of the Phenolic Profile in the Diatom *Phaeodactylum Tricornutum* Growing

- under Copper and Iron Stress. *Limnol. Oceanogr.* **2013**, *58* (1), 144–152.
<https://doi.org/10.4319/lo.2013.58.1.0144>.
- (39) Wey, L. T.; Bombelli, P.; Chen, X.; Lawrence, J. M.; Rabideau, C. M.; Rowden, S. J. L.; Zhang, J. Z.; Howe, C. J. The Development of Biophotovoltaic Systems for Power Generation and Biological Analysis. *ChemElectroChem* **2019**, *6* (21), 5375–5386.
<https://doi.org/10.1002/celec.201900997>.
- (40) Sayegh, A.; Perego, L. A.; Arderiu Romero, M.; Escudero, L.; Delacotte, J.; Guille-Collignon, M.; Grimaud, L.; Bailleul, B.; Lemaître, F. Finding Adapted Quinones for Harvesting Electrons from Photosynthetic Algae Suspensions. *ChemElectroChem* **2021**, *8* (15), 2968–2978. <https://doi.org/10.1002/celec.202100757>.
- (41) McCormick, A. J.; Bombelli, P.; Scott, A. M.; Philips, A. J.; Smith, A. G.; Fisher, A. C.; Howe, C. J. Photosynthetic Biofilms in Pure Culture Harness Solar Energy in a Mediatorless Bio-Photovoltaic Cell (BPV) System. *Energy Environ. Sci.* **2011**, *4* (11), 4699–4709.
<https://doi.org/10.1039/c1ee01965a>.
- (42) Shlosberg, Y.; Tóth, T. N.; Eichenbaum, B.; Keysar, L.; Schuster, G.; Adir, N. Electron Mediation and Photocurrent Enhancement in *Dunaliella Salina* Driven Bio-Photo Electrochemical Cells. *Catalysts* **2021**, *11* (10), 1–11.
<https://doi.org/10.3390/catal11101220>.
- (43) Liang, M. H.; Qv, X. Y.; Chen, H.; Wang, Q.; Jiang, J. G. Effects of Salt Concentrations and Nitrogen and Phosphorus Starvations on Neutral Lipid Contents in the Green Microalga *Dunaliella Tertiolecta*. *J. Agric. Food Chem.* **2017**, *65* (15), 3190–3197.

<https://doi.org/10.1021/acs.jafc.7b00552>.

- (44) Lo Presti, M.; Giangregorio, M. M.; Ragni, R.; Giotta, L.; Guascito, M. R.; Comparelli, R.; Fanizza, E.; Tangorra, R. R.; Agostiano, A.; Losurdo, M.; et al. Photoelectrodes with Polydopamine Thin Films Incorporating a Bacterial Photoenzyme. *Adv. Electron. Mater.* **2020**, *6* (7), 1–11. <https://doi.org/10.1002/aelm.202000140>.

SYNOPSIS. Biohybrid photoanodes based on living diatom microalgae onto indium thin oxide show high resistance to dryness and long durability over time.

